

# Inward rectifier K<sup>+</sup> current under physiological cytoplasmic conditions in guinea-pig cardiac ventricular cells

Keiko Ishihara, Ding-Hong Yan, Shintaro Yamamoto and Tsuguhisa Ehara

Department of Physiology, Saga Medical School, Saga 849-8501, Japan

The outward current that flows through the strong inward rectifier K<sup>+</sup> (K<sub>IR</sub>) channel generates  $I_{K1}$ , one of the major repolarizing currents of the cardiac action potential. The amplitude and the time dependence of the outward current that flows through K<sub>IR</sub> channels is determined by its blockage by cytoplasmic cations such as polyamines and Mg<sup>2+</sup>. Using the conventional whole-cell recording technique, we recently showed that the outward  $I_{K1}$  can show a time dependence during repolarization due to competition of cytoplasmic particles for blocking K<sub>IR</sub> channels. We used the amphotericin B perforated patch-clamp technique to measure the physiological amplitude and time dependence of  $I_{K1}$  during the membrane repolarization of guinea-pig cardiac ventricular myocytes. In 5.4 mM K<sup>+</sup> Tyrode solution, the density of the current consisting mostly of the sustained component of the outward  $I_{K1}$  was about 3.1 A F<sup>-1</sup> at around -60 mV. The outward  $I_{K1}$  showed an instantaneous increase followed by a time-dependent decay (outward  $I_{K1}$  transient) on repolarization to -60 to -20 mV subsequent to a 200 ms depolarizing pulse at +37 mV (a double-pulse protocol). The amplitudes of the transients were large when a hyperpolarizing pre-pulse was applied before the double-pulse protocol, whereas they were small when a depolarizing pre-pulse was applied. The peak amplitudes of the transients elicited using a hyperpolarizing pre-pulse were 0.36, 0.63 and 1.01 A F<sup>-1</sup>, and the decay time constants were 44, 14 and 6 ms, at -24, -35 and -45 mV, respectively. In the current-clamp experiments, a phase-plane analysis revealed that application of pre-pulses changed the current density at the repolarization phase to the extents expected from the changes of the  $I_{K1}$  transient. Our study provides the first evidence that an outward  $I_{K1}$  transient flows during cardiac action potentials.

(Received 1 November 2001; accepted after revision 12 February 2002)

**Corresponding author** K. Ishihara: Department of Physiology, Saga Medical School, 5-1-1 Nabeshima, Saga 849-8501, Japan.  
Email: keiko@post.saga-med.ac.jp

The strong inward rectifier K<sup>+</sup> (K<sub>IR</sub>) channel provides one of the major components of the repolarizing outward current,  $I_{K1}$ , in the cardiac action potential (AP).  $I_{K1}$  exhibits voltage- and time-dependent changes because of the blocking kinetics exerted by the intracellular polyamines and Mg<sup>2+</sup> (Matsuda *et al.* 1987; Vandenberg, 1987; Ficker *et al.* 1994; Lopatin *et al.* 1994, 1995; Fakler *et al.* 1995; Ishihara *et al.* 1996; Yamashita *et al.* 1996; Ishihara, 1997). Recently, we demonstrated that these blocking kinetics produce a transient outward current (outward  $I_{K1}$  transient) of significant amplitude on repolarization (-20 to -80 mV) following a large depolarizing pulse (>0 mV; Ishihara & Ehara, 1998). In estimating the amplitude of  $I_{K1}$  during cardiac APs in the model calculation, a time-independent rectification has been assumed, neglecting the aforementioned time-dependent kinetics of the K<sub>IR</sub> channel (Di Francesco & Noble, 1985; Luo & Rudy, 1994). However, it is expected that the time-dependent kinetics of the K<sub>IR</sub> channel would cause a dynamic change in the outward component of  $I_{K1}$  during the repolarization phase of cardiac APs.

The fast rising phase of the outward transient was explained by an instantaneous but partial relief from the magnesium-induced block (Mg<sup>2+</sup> block; see also Ishihara *et al.* 1989), and the subsequent time-dependent decay phase by a delayed polyamine-induced block (polyamine block). According to this view, the outward  $I_{K1}$  transient as well as the steady-state amplitude of outward  $I_{K1}$  should depend on the intracellular concentrations of both polyamines and Mg<sup>2+</sup>. However, the concentrations of cytoplasmic polyamines have not been controlled in our previous whole-cell recordings using the conventional ruptured-patch method. Although polyamine molecules (spermine and spermidine) are abundantly present in the cytoplasm, where they are bound to large molecules such as RNA, proteins and ATP (Watanabe *et al.* 1991), dialysis of the intracellular milieu with an artificial pipette solution might have altered the concentrations of cytoplasmic polyamines, thus influencing the recorded  $I_{K1}$ . Indeed, when we measured the inward rectifier K<sup>+</sup> current from a cultured fibroblast cell line using the conventional patch-clamp method, a washout of polyamines was strongly suggested

by a change in the time-dependent gating kinetics (Ishihara, 1997). Although such effects were not obvious in cardiac myocytes, as we have discussed in previous work (Ishihara & Ehara, 1998), there was no proof that a washout of polyamines did not influence the outward  $I_{K1}$  transients. Furthermore, while the free  $Mg^{2+}$  concentration in the pipette solution used in the previous whole-cell recordings was controlled using EDTA to mimic that in intact cardiac cells (0.5–1 mM; Murphy *et al.* 1991), the actual free  $Mg^{2+}$  concentration inside the cells during dialysis might not necessarily have been close to that in the pipette solution.

In order to extrapolate the gating kinetics of the  $K_{IR}$  channel to the cardiac AP under physiological conditions, we attempted to measure  $I_{K1}$  in the presence of physiological concentrations of cytoplasmic multivalent cations functioning as  $K_{IR}$  channel blockers. To this end, we used the amphotericin B perforated-patch clamp method, a method that was expected to prevent the washout of intracellular multivalent cations.

## METHODS

### Isolation of single ventricular cells

The method used to isolate single ventricular cells from the adult guinea-pig heart was essentially the same as that described previously (Powell *et al.* 1980; Isenberg & Klockner, 1982). Female guinea-pigs (250–400 g) were deeply anaesthetised by intraperitoneal injection of an overdose of sodium pentobarbitone (100–150 mg kg<sup>-1</sup>). Under artificial respiration, the aorta was cannulated *in situ* to start coronary perfusion with Tyrode solution. The heart was then excised and mounted on a Langendorff-type apparatus to be further perfused with a calcium-free Tyrode solution for 5 min, and with the same solution containing 0.5 mg ml<sup>-1</sup> collagenase (Wako Pure Chemical Industries, Osaka, Japan) for another 10–13 min at 37°C. After treatment with the enzyme, the cells were dissociated in a modified Kraft-Brühe (KB) solution (Isenberg & Klockner, 1982) and stored in the same solution at 4°C until later use. All procedures using animals were approved by the ethical committee of animal use of Saga Medical School.

### Solutions

The Tyrode solution contained (mM): NaCl 140, KCl 5.4, MgCl<sub>2</sub> 0.5, CaCl<sub>2</sub> 1.8, NaH<sub>2</sub>PO<sub>4</sub> 0.33, glucose 5.5 and Hepes 5, pH 7.4 with NaOH. The modified KB solution contained (mM): potassium glutamate 70, KCl 30, KH<sub>2</sub>PO<sub>4</sub> 10, MgCl<sub>2</sub> 1, taurine 20, EGTA 0.3, glucose 10 and Hepes 10, pH 7.2 with KOH. The Tyrode solution was used as the external solution in all electrophysiological experiments. In voltage-clamp experiments, nifedipine (2 μM; Sigma) and E4031 (5 μM; a gift from Eisai Pharmaceuticals, Tokyo, Japan) were added to inhibit the L-type Ca<sup>2+</sup> current ( $I_{Ca,L}$ ) and the rapidly activating delayed rectifier K<sup>+</sup> current ( $I_{Kr}$ ), respectively. To suppress the slowly activating delayed rectifier K<sup>+</sup> current ( $I_{Ks}$ ), chromanol 293B (50 μM; a gift from Hoechst Marion Roussel, Frankfurt, Germany) was also used. It has been demonstrated that E4031 and 293B do not affect  $I_{K1}$  at these concentrations (Sanguinetti & Jurkiewicz, 1990; Bosch *et al.* 1998). The pipette solution used in the perforated-patch recordings contained (mM): potassium gluconate 125, KCl 15, NaCl 10, CaCl<sub>2</sub> 1, and Hepes 5, pH 7.2 with KOH. Amphotericin B (Wako Pure Chemical Industries) stock solution (30 mg ml<sup>-1</sup> in DMSO) was

diluted with this pipette solution (final concentration, 300 μg ml<sup>-1</sup>) with the aid of sonication. Since the aqueous pores made by a polyene antibiotic amphotericin B are reported to be impermeable to divalent cations but to pass monovalent ions (Kleinberg & Finkelstein, 1984), the composition of K<sup>+</sup>, Na<sup>+</sup> and Cl<sup>-</sup> ions in the pipette solution was made similar to that in cardiac cells (Sheu & Fozzard, 1982; Tajima *et al.* 1996). We included 1 mM Ca<sup>2+</sup> in this solution so that spontaneous rupture of the perforated-patch membrane could be immediately recognised via cell contracture. The pipette solution used in the conventional whole-cell recordings contained (mM): KCl 30, potassium aspartate 85, KH<sub>2</sub>PO<sub>4</sub> 10, K<sub>2</sub>ATP 2, K<sub>2</sub>EDTA 2, MgCl<sub>2</sub> 5 and Hepes 5, pH 7.2 with KOH. The free  $Mg^{2+}$  concentration in this solution was calculated to be approximately 1 mM (Fabiato & Fabiato, 1979).

### Recording techniques

Whole-cell currents and APs were recorded using the amphotericin B perforated patch-clamp technique (Horn & Marty, 1988; Rae *et al.* 1991) with a patch-clamp amplifier (CEZ-2300, Nihon Koden, Tokyo, Japan, or Axopatch 200B, Axon Instruments, Union City, CA, USA). Whole-cell currents were also recorded by the conventional ruptured patch-clamp method (Hamill *et al.* 1981). Patch electrodes were made from Pyrex glass capillary tubes (Narishige, Tokyo, Japan). The resistances of the electrodes were 2–4 MΩ when filled with the pipette solutions. Stimulations and acquisitions of voltage and current signals were performed by pCLAMP software (version 7, Axon Instruments) on a Pentium PC through a 12-bit A/D-converter (Digidata 1200A, Axon Instruments). The isolated ventricular cells placed in the recording chamber were superfused continuously with the external solution at 35–36°C. To monitor the series resistance ( $R_s$ ) and to determine the cell membrane capacitance ( $C_m$ ), the capacity transients were recorded periodically during experiments using ± 5 mV voltage steps applied following a pre-pulse to 0 mV. The holding potential was set at the resting potential measured in each experiment. We verified that polyamines did not pass through the perforated-patch membrane by confirming that inclusion of spermine (500 μM) in the pipette solution had no obvious effects on  $I_{K1}$  in the perforated-patch recording, in contrast to the strong blocking effects on  $I_{K1}$  observed in the conventional whole-cell recording (data not shown).

### Data analysis

Based on the measurements of the liquid junction potentials between the Tyrode and the pipette solutions, the actual pipette potentials ( $V_p$ ) were assumed to be more negative than the recorded  $V_p$  by about -13 and -10 mV in the perforated-patch and the conventional configurations, respectively. Thus, the recorded  $V_p$  values were corrected by these amounts. To obtain the  $R_s$  values, the capacitive currents were fitted with a single exponential curve (Fig. 1B, inset) to determine the amplitude of the current jump ( $I_{in}$ ) at the onset of the voltage step ( $\Delta V_p$ ) from the time zero value of the exponentials. The relationship,  $R_s = \Delta V_p / I_{in}$ , was used to calculate  $R_s$ . The  $C_m$  values were obtained from the time constant ( $\tau$ ) of the capacitive transients,  $R_s$  and the membrane resistance ( $R_m$ ) using the relationship,  $C_m = \tau \times (1/R_s + 1/R_m)$ . During voltage-clamp experiments, we could usually compensate for  $R_s$  by only 40–60% using the circuit incorporated in the patch-clamp amplifier (Marty & Neher, 1995). Thus, the remaining  $R_s$ -related voltage error was corrected using the equation,  $V_m = V_p - R_s^* \times I$ , where  $R_s^*$  is the amount of  $R_s$  that remains uncompensated. The  $R_s$ -related voltage error under current-clamp conditions with current injection (Fig. 5A) was also compensated for by using the aforementioned equation. To

obtain the  $I-V_m$  relationships shown in Figs 1 and 2, the amplitude of inward currents was measured at their peak. The chord conductance values shown in Fig. 6B were obtained as  $I/(V_m - V_{rev})$ , where  $V_{rev}$  is the reversal potential of the current. Fitting of current traces to a single exponential function was carried out using pCLAMP software. Statistical values are given as the mean  $\pm$  S.E.M. (where  $n$  is the number of cells). In the figures, the pulse protocols are indicated by the  $V_p$  values. The horizontal dotted lines superimposed on the current traces indicate the zero-current level.

### Model calculation

The amplitudes of the background sodium current ( $I_{Na,b}$ ) and the  $Na^+K^+$  pump current ( $I_{NaK}$ ) shown in Fig. 6A were calculated using the formula described by Luo & Rudy (1994) at the

extracellular and intracellular concentrations of  $Na^+$  and  $K^+$  we used in this study. The calculation of the effects of pre-pulses on AP,  $I_{Ks}$  and  $I_{Kr}$  (Fig. 7) were performed according to the Luo-Rudy model of a mammalian ventricular AP (Luo & Rudy, 1994) and its modifications (Zeng *et al.* 1995; Viswanathan *et al.* 1999; Faber & Rudy, 2000), using Microsoft Visual BASIC (version 6). Briefly, the differential equation,  $dV_m/dt = -(1/C_m)(I_m + I_{stim})$ , was solved, where  $I_{stim}$  is the stimulus current and  $I_m$  is the sum of all ionic currents through the membrane. To simulate the pre-pulse effects, a depolarizing ( $-2.7 A F^{-1}$ , 50 ms) or a hyperpolarizing ( $16 A F^{-1}$ , 50 ms) current was added before applying  $I_{stim}$  ( $-65 A F^{-1}$ ,  $< 0.5$  ms). The extracellular and intracellular concentrations of  $Na^+$  and  $K^+$  were fixed at the values we used in this study. The results of calculation at each pre-pulse condition (without or with

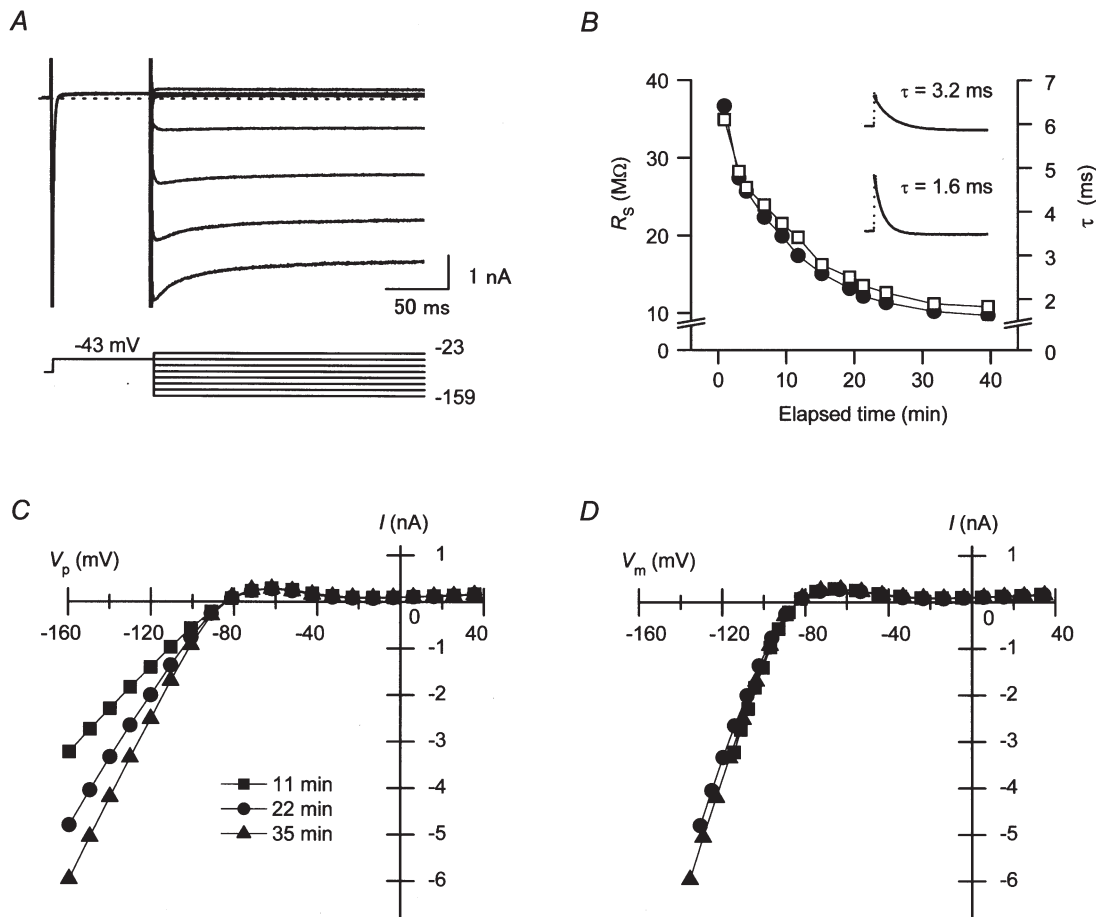


**Figure 1.**  $I_{K1}$ , a major repolarizing current in the cardiac action potential (AP), recorded from a guinea-pig ventricular cell using the amphotericin B perforated-patch method

A, representative current traces obtained using the perforated-patch method. Currents were recorded about 35 min after obtaining a gigaseal. The external solution contained nifedipine, chromanol 293B and E4031. Currents recorded using voltage pulses from  $-159$  to  $-23$  mV in about 20 mV increments are superimposed. The holding potential was kept at the resting potential ( $-84$  mV in this cell). B, changes in series resistance ( $R_S$ ,  $\square$ ) and the time constant of the capacitive currents ( $\tau$ ;  $\bullet$ ) during the experiment. Time zero indicates when a gigaseal was obtained. Compensation for  $R_S$  was not performed using the patch-clamp amplifier to obtain these data. The inset shows examples of the fitting of a single exponential curve to the capacitive currents. The time constants of the exponentials are indicated on each trace. C, current-pipette potential ( $I-V_p$ ) relationships of the currents recorded as shown in A, at about 11 min ( $\blacksquare$ ), 22 min ( $\bullet$ ), and 35 min ( $\blacktriangle$ ) after obtaining a gigaseal. The amount of  $R_S$  compensated using the patch-clamp amplifier (CEZ-2300) was 6.5 M $\Omega$ . D, current-membrane potential ( $I-V_m$ ) relationships transformed from the  $I-V_p$  relationships shown in C. To obtain these relationships, the remaining  $R_S$ -related voltage errors were calculated using the  $R_S$  values shown in B.

a depolarizing/hyperpolarizing pre-pulse) were obtained by applying  $I_{stim}$  at a cycle length of 1 s (1 Hz) for 1 min.

## RESULTS

### Stability of $I_{K1}$ recorded using the perforated-patch method

To verify that dialysis of the intracellular milieu through the perforated-patch membrane had not altered the concentration of internal particles functioning as the intrinsic blocker of  $I_{K1}$ , we first examined whether the  $I-V_m$  relationship of  $I_{K1}$  showed any change during the experiments. Figure 1A shows a family of currents recorded from a guinea-pig ventricular cell using the amphotericin B perforated-patch method using voltage steps applied to various levels. The bath solution contained blockers of  $I_{Ca,L}$ ,  $I_{Ks}$  and  $I_{Kr}$ , and voltage pulses were applied following a pre-pulse at  $-43$  mV, which inactivated the voltage-dependent  $Na^+$  current. The recorded currents, which were obtained at about 35 min after the gigaseal formation, exhibited a strong inward rectification. The small outward currents showed no significant time dependence, while the large inward currents showed a fast activation phase followed by a slow inactivation phase. These two phases of the inward currents are the characteristics of the cardiac  $I_{K1}$  (Biermans *et al.* 1987; Ishihara *et al.* 1989). In our perforated-patch experiments using amphotericin B, the value of  $R_s$  usually decreased continuously at a slow speed (Fig. 1B). When the amount of  $R_s$  compensated for using the patch-clamp amplifier was kept constant, the amplitude of inward currents increased concurrently, as shown by the  $I-V_p$  relationships (Fig. 1C). When these  $I-V_p$  relationships were transformed to  $I-V_m$  relationships by calculating the  $R_s$ -related voltage errors (see Methods), they became

similar to each other (Fig. 1D). This finding indicates that the measured currents consisting mostly of  $I_{K1}$  were stable, and that the particles causing the strong inward rectification of  $I_{K1}$  remained in the intracellular space throughout the perforated-patch experiment. In all cells examined, the corrected  $I-V_m$  relationships of the currents thus recorded remained nearly unchanged throughout the experiments ( $n = 6$ ).

### Density of $I_{K1}$ in guinea-pig ventricular cells

Since  $R_s$  did not fluctuate, but showed only a slow change during the perforated-patch clamp experiments (Fig. 1B), we considered it reliable enough to obtain  $I-V_m$  relationships by estimating the  $R_s$ -related voltage error using the  $R_s$  values measured periodically during experiments. The  $I-V_m$  relationships of the currents thus obtained from different cells are shown in Fig. 2A. The mean value of the  $V_{rev}$  of the relationships was  $-83.1 \pm 0.6$  mV ( $n = 9$ ). The current amplitudes expressed relative to the cell capacitance were similar to each other, suggesting that the ventricular cells possess a similar density of  $I_{K1}$ . Figure 2B shows the relationships between  $V_m$  in the physiological range and the outward-current density. The hump of outward current flowing at less positive voltages is characteristic of  $I_{K1}$  in cardiac cells (Matsuda & Noma, 1984; Ishihara & Ehara, 1998). The maximum value of the outward current was  $3.1 \pm 0.1$  A F $^{-1}$  at  $-63.5 \pm 1.1$  mV ( $n = 9$ ).

### Outward $I_{K1}$ transient observed in perforated-patch recordings

The experiments carried out using the conventional ruptured-patch-clamp method have indicated that the outward current of cardiac  $I_{K1}$  can show a time dependence that is most likely to be due to competition between intracellular  $Mg^{2+}$  and polyamines for blocking  $K_{IR}$

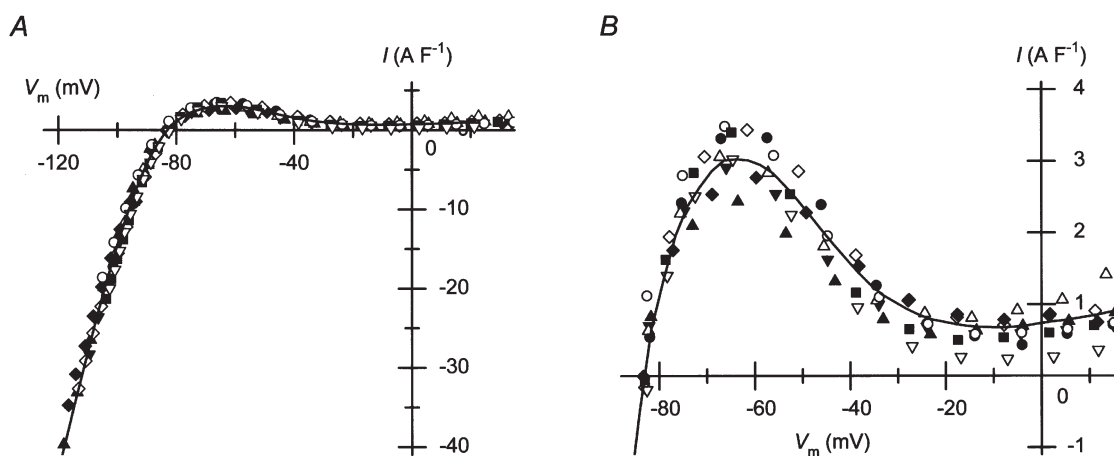


**Figure 2. Density of  $I_{K1}$  in guinea-pig ventricular cells measured using perforated-patch recordings**

A,  $I-V_m$  relationships of the currents obtained as described in Fig. 1 from different cells. Current amplitudes are expressed as relative to the cell capacitance. The capacitance of the ventricular cells used to obtain the data was  $150 \pm 11$  pF ( $n = 9$ ). The continuous curve indicates the average relationship. B, outward-current density in the physiological voltage range. The plot shown in A was expanded. The continuous line is the average relationship also shown in A.

channels (Ishihara & Ehara, 1998). When the intracellular solution contained about 1 mM free  $Mg^{2+}$ , the outward current recorded exhibited a clear transient that was presumably due to an instantaneous relief of the  $Mg^{2+}$  block and the slow re-block of  $K_{IR}$  channels by polyamine. The current traces shown in Fig. 3 indicate that the transient component of the outward  $I_{K1}$  was indeed observed using the perforated-patch method. When a large depolarizing pulse was applied after a hyperpolarizing pre-pulse to

-120 mV, a transient component was observed in the outward currents during the subsequent repolarizing steps to -42, -33 and -23 mV (Fig. 3A, left column). The amplitude of the transients became smaller when the pre-pulse was not applied (Fig. 3A, middle column), and it became negligible when using a depolarizing pre-pulse to -42 mV (Fig. 3A, right column). The maximum amplitude of the inward currents was not affected by the pre-pulses (Fig. 3A, panels in the lower row), indicating that a change

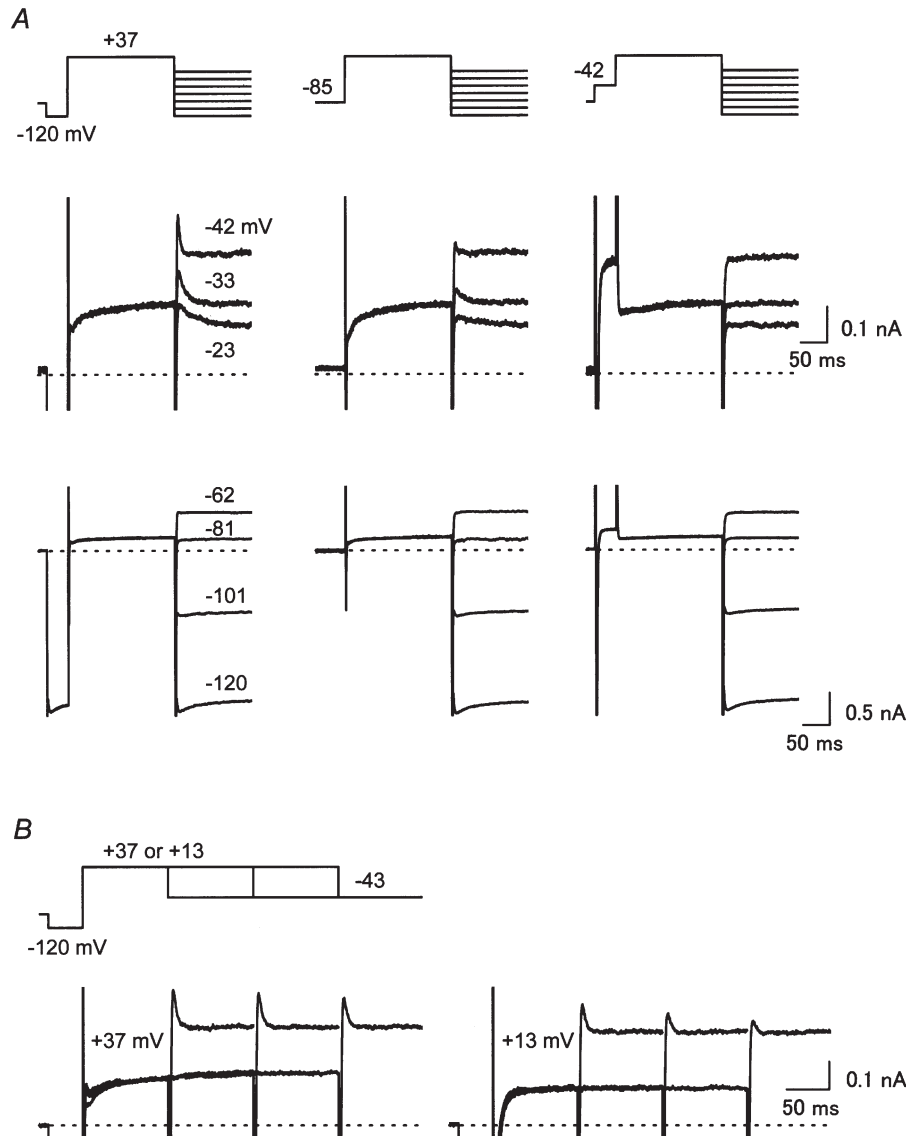


**Figure 3. Outward  $I_{K1}$  transients observed using perforated-patch recording**

A, pre-pulse dependence of the transient outward currents observed during repolarizing voltage steps applied subsequent to a depolarizing pulse (+37 mV, 200 ms). A hyperpolarizing (-120 mV) or a depolarizing (-42 mV) pre-pulse was applied in the left or the right column, respectively. Currents recorded using repolarizing steps at voltages between -23 and -42 mV are superimposed in the middle row, and those at below -62 mV are superimposed in the lower row. B, dependence of the amplitude of the transient outward current on the duration of the depolarizing pulse (left panel, +37 mV, right panel, +13 mV). Currents recorded using depolarizing pulses of different durations (100, 200 and 300 ms) are superimposed in each panel. Currents shown in this figure were recorded from the same cell placed in an external solution containing nicaidipine, chromanol 293B and E4031. The holding potential was set at the resting potential (-85 mV in this cell). Inward currents observed during hyperpolarizing pre-pulses are truncated in the middle row of A and B.

in the  $R_S$  value was not involved in the generation of the transients. This pre-pulse dependence of the repolarization-evoked transients is comparable to that of the outward  $I_{K1}$  transients observed using the ruptured-patch method. It is suggested that  $Mg^{2+}$  blockade during depolarization to +37 mV was facilitated by opening  $K_{IR}$  channels before the depolarization, and was hindered by closing the channels through the polyamine block before the depolarization. Figure 3B shows that the peak amplitude of the outward transient became smaller as the duration of the depolarizing pulse to +37 mV was prolonged. This attenuation of the

transient occurred faster when the depolarizing pulse was applied to a more negative voltage (+13 mV). These findings were also consistent with the behaviour of the outward  $I_{K1}$  transient observed in ruptured-patch recordings. It is considered that the re-equilibration of  $K_{IR}$  channels from the  $Mg^{2+}$  block to the polyamine block occurs even during depolarization, with a slower speed at more positive voltages. These findings were consistent in all 15 cells we examined, suggesting that the gating mechanisms of  $K_{IR}$  channels inferred from the ruptured-patch experiments hold true under physiological cytoplasmic conditions.

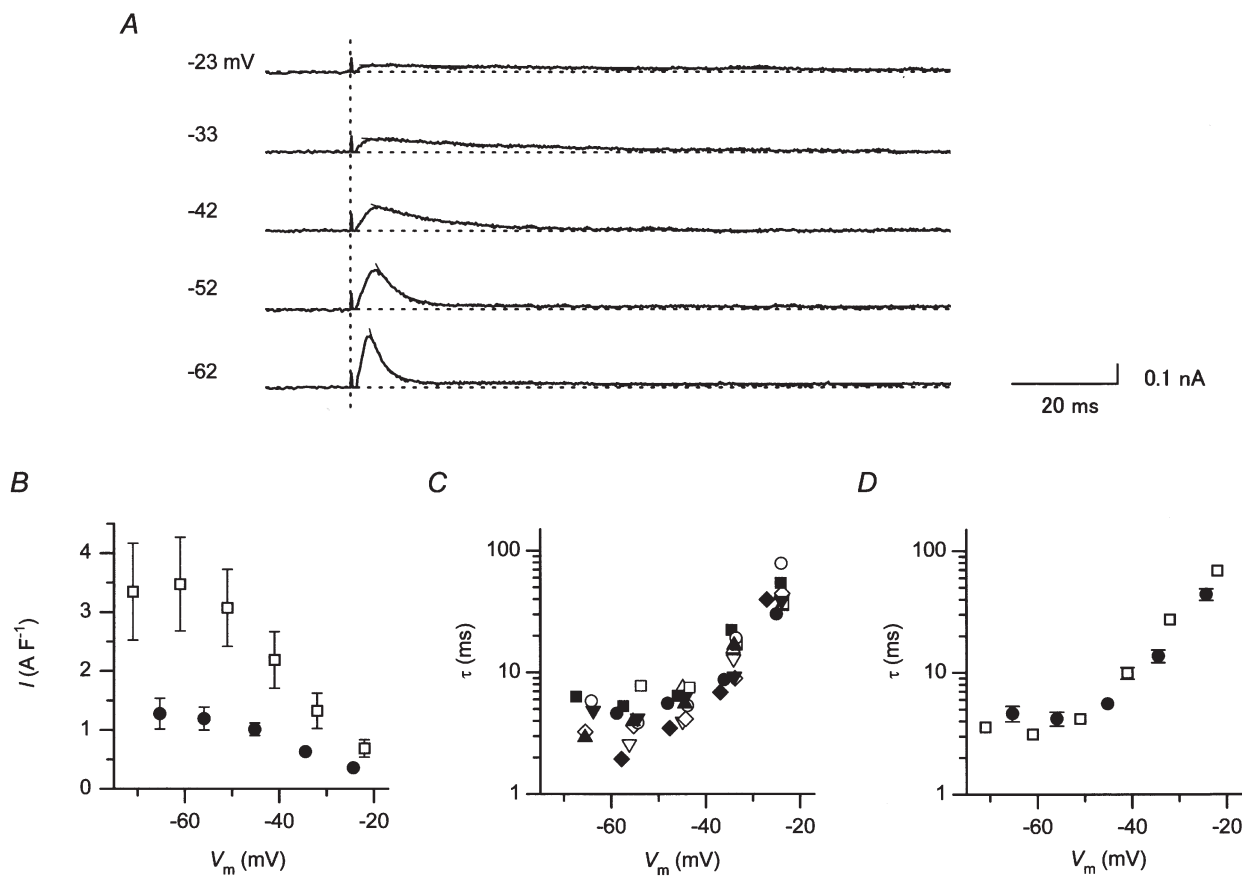


**Figure 4. Time and voltage dependences of the outward  $I_{K1}$  transient, as observed by perforated-patch recordings**

A, isolated transient components of the outward  $I_{K1}$  observed during repolarizing voltage steps. Transient currents were evoked using a hyperpolarizing pre-pulse, as illustrated in Fig. 3A (left), and were isolated by digitally subtracting the sustained current components recorded using a depolarizing pre-pulse (Fig. 3A, right). The vertical dotted line indicates the time points when repolarizing steps were given. The numerals on the left of each trace indicate  $V_p$  at the repolarizing pulses. Fits of a single exponential curve to the decaying phase of the current components are also given. B, peak amplitudes of the transients plotted against  $V_m$  during repolarizing voltage steps. Plotted are the data obtained by perforated patch using a 200 ms depolarizing pulse to +37 mV ( $\bullet$ ,  $n = 5$ ), and those by the ruptured patch using a 100 ms depolarizing pulse to +30 mV ( $\square$ ,  $n = 7$ ). The pipette solution used in ruptured-patch recording contained about 1 mM free  $Mg^{2+}$  and no polyamines. The values are the mean values, and the vertical lines indicate S.E.M. The S.E.M. is not shown where the value was smaller than the symbol. C, time constants of the decaying phase of the outward  $I_{K1}$  transients. Data obtained from 10 perforated-patch experiments are plotted against  $V_m$  at the repolarizing steps. Different symbols indicate different experiments. D, comparison of the decay time constants obtained by perforated patch clamp ( $\bullet$ ) and by ruptured patch clamp ( $\square$ ). The mean values are shown (perforated patch,  $n = 10$ ; ruptured patch,  $n = 8$ ).

### Time and voltage dependence of the outward $I_{K1}$ transient under physiological cytoplasmic conditions

Figure 4A shows the isolated outward  $I_{K1}$  transients induced by repolarization of different amplitudes in the perforated-patch recording. The amplitude of the transients became larger as the voltage in the repolarizing steps was made more negative, closer to the resting potential (Fig. 4B). This observation is consistent with the view that the more negative the voltage is, the larger the extent of the relief of  $Mg^{2+}$  block becomes. The peak amplitudes of the transients measured using a depolarizing pulse to +37 mV for 200 ms were  $0.36 \pm 0.04$ ,  $0.63 \pm 0.06$  and  $1.01 \pm 0.11$  A  $F^{-1}$  at  $-24 \pm 0.09$ ,  $-34 \pm 0.2$  and  $-45 \pm 0.43$  mV, respectively

( $n = 4$ ). Like those observed in the ruptured-patch experiments, the rate of the decay was increased by making the voltage during the repolarization more negative (Fig. 4A). It is considered that the polyamine block underlying the decay of the outward current is accelerated at less positive voltages because the competition with the  $Mg^{2+}$  block is reduced (Ishihara & Ehara, 1998). The time course of the current decay could be fitted by a single exponential function (Fig. 4A). The voltage dependence of the time constants are shown in Fig. 4C. The time constants under the perforated patch-clamp measurement were  $44.2 \pm 4.9$ ,  $13.7 \pm 1.6$  and  $5.6 \pm 0.4$  ms at  $-24.3 \pm 0.4$ ,  $-34.5 \pm 0.4$  and  $-45.2 \pm 0.5$  mV ( $n = 10$ ), respectively. In our previous whole-cell recordings, the amplitude of

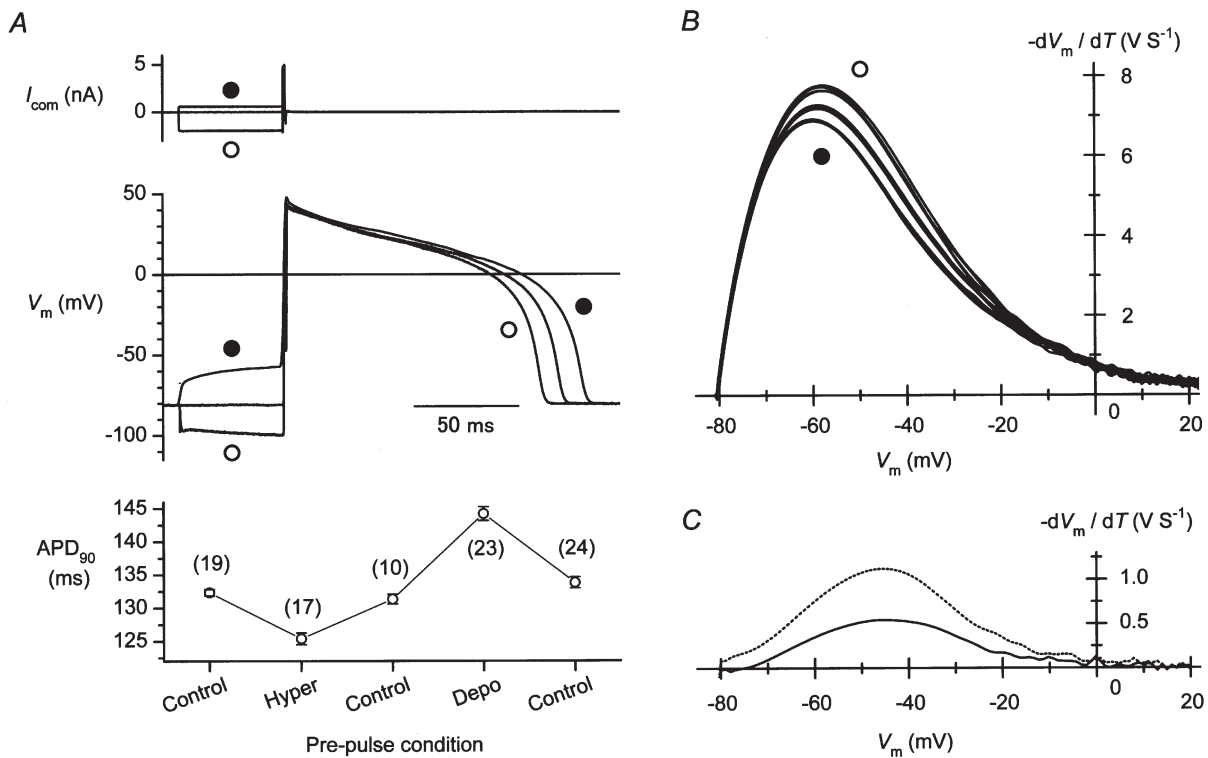


**Figure 5. Effects of a hyperpolarizing or a depolarizing pre-pulse on AP duration (APD) and the net current density during AP repolarization**

A, changes in the APD observed using a depolarizing (●) or hyperpolarizing (○) current pre-pulse. Command pulses (5 nA, 0.9 ms) without or with a pre-pulse of appropriate amplitude were applied continuously at 1 Hz to elicit APs. The same pre-pulse condition was used for about 30 s to record APs. The pre-pulse condition was changed chronologically in the following order: 'without a pre-pulse' (Control), 'with a hyperpolarizing pre-pulse' (Hyper), Control, 'with a depolarizing pre-pulse' (Depo) and Control. Representative AP records observed at each pre-pulse condition are shown. The plot in the bottom panel shows APD<sub>90</sub> at each pre-pulse condition. Each symbol represents the mean  $\pm$  S.E.M. The number of records analysed to obtain the data is indicated in parentheses. B, phase-plane diagrams obtained from the repolarization phase of the APs. The  $-dV_m/dt$  values calculated from the APs are plotted against  $V_m$ . Five representative relationships are shown for each pre-pulse condition. APs were digitally filtered at 200 Hz before calculation. Note that the unit  $V S^{-1}$  is equivalent to  $A F^{-1}$ . The amplitude of the outward current decreased with the depolarizing (●) and increased with the hyperpolarizing (○) pre-pulse. C, changes in the current density at the repolarization phase caused by using pre-pulses. Shown are the difference between  $-dV_m/dt$  (net current density)– $V_m$  relationships obtained with depolarizing (●) and hyperpolarizing (○) pre-pulses (dotted line), and that between the relationships obtained with and without a depolarizing pre-pulse (continuous line).

outward  $I_{K1}$  transients varied among the experiments (Ishihara & Ehara, 1998). Since the previous study was performed at room temperature in order to suppress  $I_{Ks}$ , we re-examined the  $I_{K1}$  transients using the ruptured-patch method at physiological temperatures, with a pipette solution containing about 1 mM free  $Mg^{2+}$  but no polyamines (Fig. 4B). Although the voltage dependences of the amplitude of the transients were similar between the two methods, the amplitudes of the transients measured using the perforated-patch method were obviously less variable, and the mean values of the amplitudes were smaller than those obtained using the ruptured-patch method. In contrast, the time constants obtained with the perforated patch recordings (Fig. 4D, ●) were comparable to those found in the ruptured-patch recordings (Fig. 4D, □).

### Outward $I_{K1}$ transient during cardiac APs

In the experiment shown in Fig. 5, we confirmed whether the outward  $I_{K1}$  transient flows during the cardiac APs. To this end, the membrane voltage was temporally (50 ms) changed by injecting a depolarizing or a hyperpolarizing current before eliciting APs. The resulting changes in the relationship between  $V_m$  and the rate of the change in  $V_m$  ( $dV_m/dt$ ) at the repolarization phase of the AP records (the phase-plane diagram) were analysed. When the AP duration (APD) was measured at the level of 90% repolarization (APD<sub>90</sub>), the mean value was found to be shorter with a hyperpolarizing pre-pulse than the control, while it was longer with a depolarizing pre-pulse (Fig. 5A, bottom). These observations are in line with the changes in the flow of the outward  $I_{K1}$  transient caused by using the pre-pulses (Fig. 3A). The phase-plane diagram at the final repolarization phase indicated that the  $-dV_m/dt$  value,

which is equivalent to the net current density that flows during APs, became distinctly large with a hyperpolarizing pre-pulse (Fig. 5B, ○) and small with a depolarizing pre-pulse (Fig. 5B, ●). These changes in the current density were consistent with the pre-pulse dependence of the outward  $I_{K1}$  transient (Fig. 3A). The differences in the net outward currents observed using different pre-pulse conditions are depicted in Fig. 5C. The maximum amplitude of the difference current obtained with hyperpolarizing and depolarizing pre-pulses was about  $1.1 \text{ A F}^{-1}$  at around  $-45 \text{ mV}$  (dotted line). This value was comparable to the maximum amplitude of the transients observed in the voltage-clamp experiments at around the corresponding voltage (Fig. 4B), supporting the view that these changes are largely attributable to the flow of the outward  $I_{K1}$  transient during the repolarization phase of the actual APs. The flow of the  $I_{K1}$  transient during the control AP, estimated from the change induced by using the depolarizing pre-pulse (continuous line), was about  $0.5 \text{ A F}^{-1}$  at  $-45 \text{ mV}$ .

## DISCUSSION

In this study, we utilised the amphotericin B perforated-patch method to measure  $I_{K1}$  in guinea-pig cardiac ventricular cells in the presence of physiological concentrations of cytoplasmic multivalent cations including polyamines and  $Mg^{2+}$ . In biological membranes, amphotericin B has been shown to form pores that pass monovalent ions but exclude multivalent ions such as  $Ca^{2+}$  and  $Mg^{2+}$  (Kleinberg & Finkelstein, 1984). Although organic multivalent cations (polyamines) were not likely to permeate amphotericin B pores, we tested their ability to do so, since the shortest diameter of spermine and spermidine molecules ( $\sim 4 \text{ \AA}$ ) is

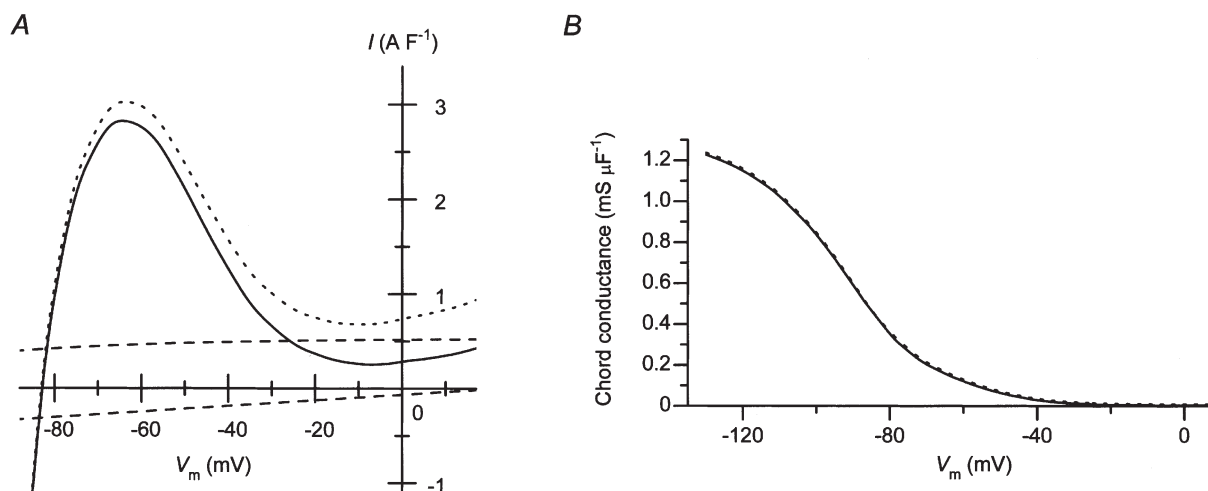


**Figure 6. Estimation of the steady-state amplitude of  $I_{K1}$  in cardiac ventricular cells**

A, estimated density of the outward  $I_{K1}$  in the steady state (continuous line). The amplitudes of the background  $Na^+$  current ( $I_{Na,b}$ ; inward current shown by the dashed line) and the  $Na^+K^+$  pump current ( $I_{NaK}$ ; outward current shown by the dashed line) were subtracted from the average amplitudes of the measured currents shown in Fig. 2A (shown by the dotted line in this plot). B, voltage dependence of the chord conductance of the estimated  $I_{K1}$  (continuous line). The chord conductance obtained from the average  $I-V_m$  relationship shown in Fig. 2A is also plotted with a dotted line.



smaller than that of the amphotericin B pores ( $\sim 8 \text{ \AA}$ ; Holz & Finkelstein, 1970). The inclusion of spermine in the pipette solution had no obvious effect on  $I_{K1}$  in the perforated-patch recording, in contrast to the strong blocking effects observed in the ruptured-patch recording (data was not shown). We thus considered that polyamines do not pass through the perforated-patch membrane.

Using the perforated-patch recording, we first obtained the  $I$ - $V_m$  relationship of currents consisting mostly of  $I_{K1}$  (Figs 1 and 2). In measuring the currents, the transient component of outward  $I_{K1}$  was eliminated by using a depolarizing pre-pulse to  $-43 \text{ mV}$  (Fig. 3), which was also employed to inactivate the voltage-dependent  $\text{Na}^+$  current. The amplitude of inward currents was measured at their peak, before the slow inactivation of  $I_{K1}$  proceeded, so as to evaluate the blockage (inward rectification) of  $I_{K1}$  caused by cytoplasmic particles. It has been shown that the inactivation of inward  $I_{K1}$ , which occurs at hyperpolarized voltage levels (Fig. 1A), is mainly caused by the blockage of  $K_{IR}$  channel by external  $\text{Na}^+$  and divalent cations (Biermans *et al.* 1987; Kubo *et al.* 1993). The recorded currents should also contain currents other than  $I_{K1}$ , such as  $I_{\text{NaK}}$  (Nakao & Gadsby, 1989) and  $I_{\text{Na,b}}$  (Kiyosue *et al.* 1993). Although the amplitudes of these currents are negligible compared to that of the inward  $I_{K1}$ , they contribute to the outward current flowing in the physiological voltage range. The amplitudes of  $I_{\text{NaK}}$  and  $I_{\text{Na,b}}$  reconstructed using mathematical models are shown in Fig. 6A (dashed lines; for the formula reconstructing  $I_{\text{NaK}}$  and  $I_{\text{Na,b}}$ , see Luo & Rudy, 1994). Since the steady-state  $I$ - $V_m$  relationship of outward  $I_{K1}$  under physiological cytoplasmic conditions has not yet been obtained, we attempted to estimate it by subtracting these reconstructed currents from the measured current (Fig. 6A,

continuous line). Ideally, a selective blocker of  $I_{K1}$  should be used to isolate  $I_{K1}$ . However, such a compound has yet to be discovered. Although external  $\text{Ba}^{2+}$  is often used to block currents through  $K_{IR}$  channels, a high concentration of  $\text{Ba}^{2+}$  is required to suppress the outward current of  $I_{K1}$  (Hirano & Hiraoka, 1988), which also suppresses the cardiac background conductance in a concentration-dependent fashion (Ehara *et al.* 1989). The outward  $I_{K1}$  in the steady state thus estimated, flowed at voltages more negative than  $-20 \text{ mV}$ , with the peak amplitude of about  $3 \text{ A F}^{-1}$  at around  $-60 \text{ mV}$ . In Fig. 6B, the chord conductance of the estimated  $I_{K1}$  is plotted against  $V_m$  (continuous line). The relationship is analogous to the chord conductance of the measured current (dotted line), since the conductance of the subtracted currents is negligible compared to that of the inward  $I_{K1}$ . The conductance values at  $V_{\text{rev}}$  and  $-120 \text{ mV}$  (the voltage about  $40 \text{ mV}$  below  $V_{\text{rev}}$ ) were about  $0.4$  and  $1.2 \text{ mS } \mu\text{F}^{-1}$ , respectively.

When pipette solutions dialysing the intracellular milieu contained about  $1 \text{ mM}$  free  $\text{Mg}^{2+}$  in the conventional whole-cell recordings, a repolarization of the membrane induced a transient increase in outward  $I_{K1}$  in cardiac ventricular cells. The voltage-dependent behaviour of this outward  $I_{K1}$  transient could be explained by a substitution of the polyamine block in place of the  $\text{Mg}^{2+}$  block of  $K_{IR}$  channels, using a mathematical model incorporating competition between these molecules for blocking  $K_{IR}$  (Ishihara & Ehara, 1998). In this study, we demonstrated that transient outward currents that exhibited pre-pulse dependence (Figs. 3A, B) and voltage-dependent kinetics (Fig. 4) similar to the aforementioned  $I_{K1}$  transient were observed with the aid of perforated-patch recording. The findings indicated that the gating mechanisms of  $K_{IR}$

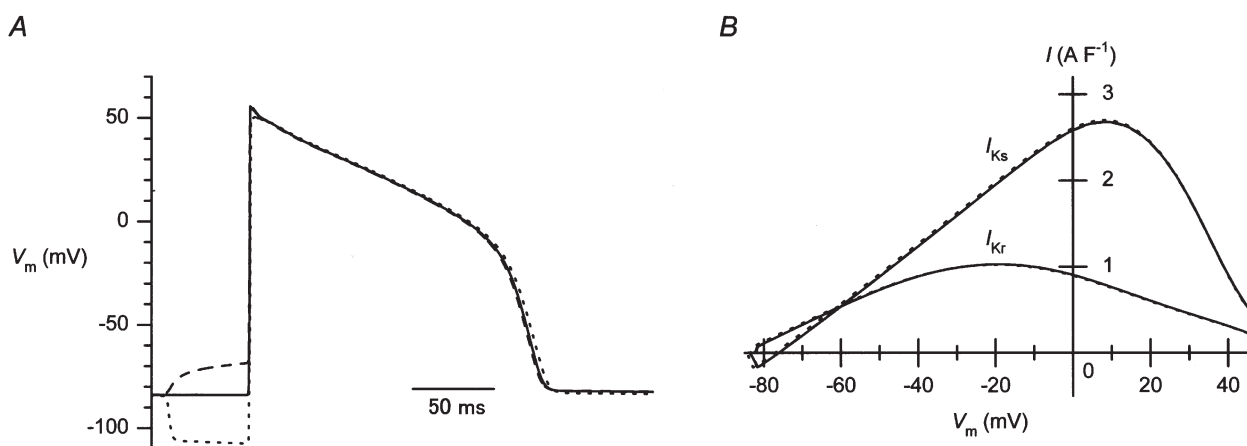


**Figure 7. Effects of pre-pulses on the slowly activating and rapidly activating delayed rectifier currents ( $I_{Ks}$  and  $I_{Kr}$  respectively) during AP repolarization, calculated using a theoretical model of a mammalian AP**

A, effects of pre-pulses on the AP reconstituted using the model calculation. A depolarizing ( $-2.7 \text{ A F}^{-1}$ ,  $50 \text{ ms}$ ) or a hyperpolarizing ( $16 \text{ A F}^{-1}$ ,  $50 \text{ ms}$ ) current was added before the stimulating current ( $I_{\text{stim}}$ ) was applied. B,  $I_{Ks}$  and  $I_{Kr}$  plotted against  $V_m$  during the repolarization phase of the reconstituted APs. The continuous line, control; dashed line, with a depolarizing pre-pulse; dotted line, with a hyperpolarizing pre-pulse.

channels deduced from the studies performed under conditions of internal dialysis are essentially applicable to the intact cells. The amplitudes of the transients observed with the aid of the perforated-patch clamp method were less variable than those recorded by the ruptured-patch recording (Fig. 4B). Using the latter method, the  $I_{K1}$  transient was sometimes much more pronounced than that observed using the perforated-patch method (e.g. Fig. 10 in Ishihara & Ehara, 1998). We consider that a washout of polyamines, molecules that compete with  $Mg^{2+}$  to block  $K_{IR}$  channels upon depolarization, might have enhanced the amplitude of the outward  $I_{K1}$  transient in the conventional whole-cell recordings, and that the amplitudes of the transients obtained by the ruptured-patch method in this study represent those recorded under physiological cytoplasmic conditions. In contrast, the decay rates of the transients measured using the two methods were similar. Although we do not have a clear explanation for this discrepancy, the amplitude of the transients might be more sensitive to the changes in the concentration of intracellular blockers than the rate constants of the current decay.

The amplitude of the  $I_{K1}$  transient flowing at the repolarization phase of the actual AP was estimated to be about  $0.5 \text{ A F}^{-1}$  at around  $-45 \text{ mV}$  in the experiment shown in Fig. 5. The current amplitude became small at voltages more negative than around  $-50 \text{ mV}$ , as we have demonstrated previously using repolarizing ramp pulses (Ishihara & Ehara, 1998). This differs from the voltage dependence of the  $I_{K1}$  transient amplitude measured using repolarizing step pulses (Fig. 4B). This is because the transient decays at a fast speed at voltages near the resting potential (Figs. 4C, D). The amplitude of the outward  $I_{K1}$  transient flowing at the AP repolarization phase should be affected by variable levels of the resting potential, the AP plateau potential and the repolarization speed, due to its unique time and voltage dependences, as we have demonstrated previously using repolarizing ramps. It should be noted, however, that the net current density during the repolarization phase of the control APs was often significantly larger (e.g. about  $7 \text{ A S}^{-1}$  at around  $-60 \text{ mV}$ ; Fig. 5B) than the sum of the amplitudes of the sustained component of  $I_{K1}$  (Figs 2B and 6A) and the outward  $I_{K1}$  transient (Fig. 4B) obtained in this study. The outward current of  $I_{K1}$  has been considered to play a major role in the final phase of the AP repolarization in rabbit cardiac ventricular cells (Shimoni *et al.* 1992; Mitcheson & Hancox, 1999). However, the difference may be explained by a substantial contribution of the slowly and the rapidly activating types of the delayed-rectifier  $K^+$  currents not only at the initial phase of repolarization, but at the final repolarization phase in guinea-pig ventricular cells. In the Luo–Rudy model of a mammalian ventricular AP, the application of pre-pulses affected significantly neither the AP duration nor the delayed-rectifier  $K^+$  currents ( $I_{Ks}$  and  $I_{Kr}$ ) that flow during the repolarization phase of the AP (Fig. 7).

When we performed in many cells the type of experiments demonstrated in Fig. 5, the size of the effects of pre-pulses on AP duration were variable. We believe that this was chiefly because pre-pulses influenced not only the  $I_{K1}$  that flows during the repolarization phase, but also the currents that flow during the plateau phase. For example, the depolarizing pre-pulse, which was kept below  $-60 \text{ mV}$  lest it should generate an AP, might have activated the delayed-rectifier  $K^+$  currents, and may have inactivated  $I_{Ca,L}$ , which provides the major inward current that maintains the plateau phase, to some extent. Since the net current is small at the plateau voltages, these changes, if any, could alter significantly the AP duration in the direction opposite to that expected from the effect of the outward  $I_{K1}$  transient. Thus, to understand the role of the dynamics of  $I_{K1}$  and the influence of the concentrations of cytoplasmic polyamines and  $Mg^{2+}$  on cardiac APs, it is useful to examine them by using a mathematical model of cardiac APs incorporating the time dependence of the outward  $I_{K1}$ . We are currently re-evaluating the blocking kinetics of polyamines and  $Mg^{2+}$  of  $K_{IR}$  channels under physiological conditions in an attempt to establish a model that will reconstruct the amplitude and time-dependence of the outward  $I_{K1}$  obtained in the present study.

## REFERENCES

- BIERMANS, G., VEREECKE, J. & CARMELIET, E. (1987). The mechanism of the inactivation of the inward-rectifying K current during hyperpolarizing steps in guinea-pig ventricular myocytes. *Pflügers Archiv* **410**, 604–613.
- BOSCH, R. F., GASPO, R., BUSCH, A. E., LANG, H. J., LI, G. R. & NATTEL, S. (1998). Effects of the chromanol 293B, a selective blocker of the slow, component of the delayed rectifier  $K^+$  current, on repolarization in human and guinea pig ventricular myocytes. *Cardiovascular Research* **38**, 441–450.
- DI FRANCESCO, D. & NOBLE, D. (1985). A model of cardiac electrical activity incorporating ionic pumps and concentration changes. *Philosophical Transactions of the Royal Society B* **307**, 353–398.
- EHARA, T., MATSUOKA, S. & NOMA, A. (1989). Measurement of reversal potential of  $Na^+$ – $Ca^{2+}$  exchange current in single guinea-pig ventricular cells. *Journal of Physiology* **410**, 227–249.
- FABER, G. M. & RUDY, Y. (2000). Action potential and contractility changes in  $[Na^+]_i$  overloaded cardiac myocytes: a simulation study. *Biophysical Journal* **78**, 2392–2404.
- FABIATO, A. & FABIATO, F. (1979). Calculator programs for computing the composition of the solutions containing multiple metals and ligands used for experiments in skinned muscle cells. *Journal of Physiology (Paris)* **75**, 463–505.
- FAKLER, B., BRANDLE, U., GLOWATZKI, E., WEIDEMANN, S., ZENNER, H.-P. & RUPPERSBERG, J. P. (1995). Strong voltage-dependent inward rectification of inward rectifier  $K^+$  channels is caused by intracellular spermine. *Cell* **80**, 149–154.
- FICKER, E., TAGLIALATELA, M., WIBLE, B. A., HENLEY, C. M. & BROWN, A. M. (1994). Spermine and spermidine as gating molecules for inward rectifier  $K^+$  channels. *Science* **266**, 1068–1072.
- HAMILL, O. P., MARTY, A., NEHER, E., SAKMANN, B. & SIGWORTH, F. J. (1981). Improved patch-clamp techniques for high-resolution current recording from cells and cell-free membrane patches. *Pflügers Archiv* **391**, 85–100.

- HIRANO, Y. & HIRAOKA, M. (1988). Barium-induced automatic activity in isolated ventricular myocytes from guinea-pig hearts. *Journal of Physiology* **395**, 455–472.
- HOLZ, R. & FINKELSTEIN, A. (1970). The water and nonelectrolyte permeability induced in thin lipid membranes by the polyene antibiotics nystatin and amphotericin B. *Journal of General Physiology* **56**, 125–145.
- HORN, R. & MARTY, A. (1988). Muscarinic activation of ionic currents measured by a new whole-cell recording method. *Journal of General Physiology* **92**, 145–159.
- ISENBERG, G. & KLOCKNER, U. (1982). Calcium tolerant ventricular myocytes prepared by preincubation in a “KB medium”. *Pflügers Archiv* **395**, 6–18.
- ISHIHARA, K. (1997). Time-dependent outward currents through the inward rectifier potassium channel IRK1. The role of weak blocking molecules. *Journal of General Physiology* **109**, 229–243.
- ISHIHARA, K. & EHARA, T. (1998). A repolarization-induced transient increase in the outward current of the inward rectifier  $K^+$  channel in guinea-pig cardiac myocytes. *Journal of Physiology* **510**, 755–771.
- ISHIHARA, K., HIRAOKA, M. & OCHI, R. (1996). The tetravalent organic cation spermine causes the gating of the IRK1 channel expressed in murine fibroblast cells. *Journal of Physiology* **491**, 367–381.
- ISHIHARA, K., MITSUIYE, T., NOMA, A. & TAKANO, M. (1989). The  $Mg^{2+}$  block and intrinsic gating underlying inward rectification of the  $K^+$  current in guinea-pig cardiac myocytes. *Journal of Physiology* **419**, 297–320.
- KIYOSUE, T., SPINDLER, A. J., NOBLE, S. J. & NOBLE, D. (1993). Background inward current in ventricular and atrial cells of the guinea-pig. *Proceedings of the Royal Society B* **252**, 65–74.
- KLEINBERG, M. E. & FINKELSTEIN, A. (1984). Single-length and double-length channels formed by nystatin in lipid bilayer membranes. *Journal of Membrane Biology* **80**, 257–269.
- KUBO, Y., BALDWIN, T. J., JAN, Y. N. & JAN, L. Y. (1993). Primary structure and functional expression of a mouse inward rectifier potassium channel. *Nature* **362**, 127–133.
- LOPATIN, A. N., MAKHINA, E. N. & NICHOLS, C. G. (1994). Potassium channel block by cytoplasmic polyamines as the mechanism of intrinsic rectification. *Nature* **372**, 366–369.
- LOPATIN, A. N., MAKHINA, E. N. & NICHOLS, C. G. (1995). The mechanism of inward rectification of potassium channels: “long-pore plugging” by cytoplasmic polyamines. *Journal of General Physiology* **106**, 923–955.
- LUO, C. H. & RUDY, Y. (1994). A dynamic model of the cardiac ventricular action potential. I. Simulations of ionic currents and concentration changes. *Circulation Research* **74**, 1071–1096.
- MARTY, A. & NEHER, E. (1995). Tight-seal whole-cell recordings. In *Single-Channel Recording*, 2nd edn, ed. SAKMANN, B. & NEHER, E. pp. 31–52. Plenum, New York.
- MATSUDA, H. & NOMA, A. (1984). Isolation of calcium current and its sensitivity to monovalent cations in dialysed ventricular cells of guinea-pig. *Journal of Physiology* **357**, 553–573.
- MATSUDA, H., SAIGUSA, A. & IRISAWA, H. (1987). Ohmic conductance through the inwardly rectifying K channel and blocking by internal  $Mg^{2+}$ . *Nature* **325**, 156–159.
- MITCHESON, J. S. & HANCOX, J. C. (1999). An investigation of the role played by the E-4031-sensitive (rapid delayed rectifier) potassium current in isolated rabbit atrioventricular nodal and ventricular myocytes. *Pflügers Archiv* **438**, 843–850.
- MURPHY, E., FREUDENRICH, C. C. & LIEBERMAN, M. (1991). Cellular magnesium and Na/Mg exchange in heart cells. *Annual Review of Physiology* **53**, 273–287.
- NAKAO, M. & GADSBY, D. C. (1989). [Na] and [K] dependence of the Na/K pump current-voltage relationship in guinea pig ventricular myocytes. *Journal of General Physiology* **94**, 539–565.
- POWELL, T., TERRAR, D. A. & TWIST, V. W. (1980). Electrical properties of individual cells isolated from adult rat ventricular myocardium. *Journal of Physiology* **302**, 131–153.
- RAE, J., COOPER, K., GATES, P. & WATSKY, M. (1991). Low access resistance perforated patch recordings using amphotericin B. *Journal of Neuroscience Methods* **37**, 15–26.
- SANGUINETTI, M. C. & JURKIEWICZ, N. K. (1990). Two components of cardiac delayed rectifier  $K^+$  current. Differential sensitivity to block by class III antiarrhythmic agents. *Journal of General Physiology* **96**, 195–215.
- SHEU, S. S. & FOZZARD, H. A. (1982). Transmembrane  $Na^+$  and  $Ca^{2+}$  electrochemical gradients in cardiac muscle and their relationship to force development. *Journal of General Physiology* **80**, 325–351.
- SHIMONI, Y., CLARK, R. B. & GILES, W. R. (1992). Role of an inwardly rectifying potassium current in rabbit ventricular action potential. *Journal of Physiology* **448**, 709–727.
- TAJIMA, Y., ONO, K. & AKAIKE, N. (1996). Perforated patch-clamp recording in cardiac myocytes using cation-selective ionophore gramicidin. *American Journal of Physiology* **271**, C524–532.
- VANDEBERG, C. A. (1987). Inward rectification of a potassium channel in cardiac ventricular cells depends on internal magnesium ions. *Proceedings of the National Academy of Sciences of the USA* **84**, 2560–2564.
- VISWANATHAN, P. C., SHAW, R. M. & RUDY, Y. (1999). Effects of  $I_{Kr}$  and  $I_{Ks}$  heterogeneity on action potential duration and its rate dependence: a simulation study. *Circulation* **99**, 2466–2474.
- WATANABE, S.-I., KUSAMA, E., GUCHI, K., KOBAYASHI, H. & IGARASHI, K. (1991). Estimation of polyamine binding to macromolecules and ATP in bovine lymphocytes and rat liver. *Journal of Biological Chemistry* **266**, 20803–20809.
- YAMASHITA, T., HORIO, Y., YAMADA, M., TAKAHASHI, N., KONDO, C. & KURACHI, Y. (1996). Competition between  $Mg^{2+}$  and spermine for a cloned IRK2 channel expressed in a human cell line. *Journal of Physiology* **493**, 143–156.
- ZENG, J., LAURITA, K. R., ROSENBAUM, D. S. & RUDY, Y. (1995). Two components of the delayed rectifier  $K^+$  current in ventricular myocytes of the guinea pig type. Theoretical formulation and their role in repolarization. *Circulation Research* **77**, 140–152.

### Acknowledgements

The authors thank Drs A. Noma and S. Matsuoka for invaluable suggestions and M. Fuchigami for secretarial work. This work was supported by the Japan Heart Foundation and an IBM Japan Research Grant, and the Scientific Research Grants from the Ministry of Education, Culture, Sports, Science and Technology of Japan.